

PROXIMATE PROPERTY AND THERMAL STABILITY CHARACTERIZATION OF CHEMICALLY ACTIVATED CARBON FOR ORGANIC FRICTION LINING MATERIALS

AUTHORS:

L. M. Akuwueke^{1*}, C. V. Ossia², and H. U. Nwosu³

AFFILIATIONS:

^{1,2,3}Department of Mechanical Engineering, University of Port Harcourt, Port Harcourt, Nigeria.

*CORRESPONDING AUTHOR:

Email: leo_akuwueke@yahoo.com

ARTICLE HISTORY:

Received: 30 May, 2024.

Revised: 13 August, 2024.

Accepted: 24 August, 2024.

Published: 20 September, 2024.

KEYWORDS:

Agrowaste materials, Activated carbon, Proximate property, Thermal stability, Characterization, Friction lining, Oxidation stability.

ARTICLE INCLUDES:

Peer review

DATA AVAILABILITY:

On request from author(s)

EDITORS:

Chidozie Charles Nnaji

FUNDING:

None

Abstract

This work studied the proximate property and thermal stability of chemically activated carbon developed from agrowaste materials for organic friction linings. The proximate property, degradation steps, optimum degradation temperature (ODT) and oxidative stability (oxidation onset temperature (OOT) and oxidation temperature (OT)) characterizations were performed on two processed samples. Coconut shell activated carbon (CSAC) and palm kernel shell activated carbon (PKSAC) were used to prepared three compositions (%vol.) and particle sizes (μm); 0% CSAC : 100% PKSAC, 50% CSAC : 50% PKSAC, and 100% CSAC : 0% PKSAC and 60, 105 and 150 μm . Thermogravimetric analysis (TGA) and modulated differential scanning calorimetry (MDSC) methods were used to perform the characterizations and results compared with two commercial brakepads (CB1 and CB2) as controls. The proximate analysis showed that 60 μm of 0% CSAC : 100% PKSAC had the best results with 6.04% moisture, 3.99% volatile matter, 84.8% fixed carbon and 4.79% ash and compared well with the commercial friction lining materials (CB1: 2.27% moisture, 2.18% volatile matter, 45.47% fixed carbon, 48.86% ash; CB2: 1.92% moisture, 1.49% volatile matter, 37.21% fixed carbon, 58.07% ash). The thermal stability of 0% CSAC : 100% PKSAC, 50% CSAC : 50% PKSAC and 100% CSAC : 0% PKSAC samples with 150 μm particle size showed percentage ODT increase of 18.3% and 15.8%; 37.1% and 34.2%; 17.8% and 15.3% when compared with CB1 and CB2 respectively. For all developed activated carbon compositions and particle sizes, the oxidation onset temperature (OOT) compared well with CB2 while oxidation temperature (OT) compared well with CB1. Overall, the developed activated carbon compositions showed suitability for organic friction lining applications.

1.0 INTRODUCTION

Friction linings are physical materials that enhance friction between solid interfaces to control motion. The materials used to produce friction materials include organic and inorganic substances such as resin, fibres, ceramics, and metals. Due to the frictional heating at the interface of two contacting surfaces in relative motion, the ability of materials used for friction linings to withstand heat due to friction without degradation is important in selecting precursors for friction linings. To replace asbestos fibres as friction linings due to their carcinogenic effects, a healthier and environmentally friendly alternative is being explored. The tracking of material physical quantity as a function of temperature is known as thermal analysis. This quantity may be heat

HOW TO CITE:

Akuwueke, L. M., Ossia, C. V., and Nwosu, H. U. "Proximate Property and Thermal Stability Characterization of Chemically Activated Carbon for Organic Friction Lining Materials", *Nigerian Journal of Technology*, 2024; 43(3), pp. 454 – 463; <https://doi.org/10.4314/njt.v43i3.7>

© 2024 by the author(s). This article is open access under the CC BY-NC-ND license

(differential scanning calorimetry - DSC), or weight (thermogravimetric analysis - TGA) [1].

The thermal degradation of organic matter and subsequent activation of its biochar yields activated carbon which is carbonaceous and porous. This activated carbon can be used to treat effluents, support catalyst, compound purification and as pollutant adsorption in gas and liquid phases [3]. These porous carbon materials have a standard diameter of $\approx 10 \mu\text{m}$ and pore size of $< 2 \text{ nm}$ for microporous activated carbon fibre [2]. The proximate properties of typical activated carbon produced at different temperature showed that at 700°C , moisture content was 12.58%, volatile 37.88%, fixed carbon 62.12% with 0% ash content [3].

Differential scanning calorimetry is a technique used to evaluate the heat required to establish a zero-temperature difference between a reference material and the substance in a heated or cooled environment at a controlled rate within a temperature regime [4]. A measure of the amount of energy evolved or absorbed in any chemical or physical transformation is determined by the heat flux recorded. The efficiency and behaviour of activated carbon regeneration processes was investigated through thermal characterization of spent coconut shell activated carbon used for the treatment of drinking water [5]. Accordingly, the different phases of thermal treatment process were examined by TGA measurement where it was concluded that the highest difference between the regenerated and unused carbon samples and the percentage mass loss recorded for spent carbon sample were obtained below 400°C [5].

The prediction of agro-wastes bioenergy characteristics by TGA was studied by a group of researchers. The proximate and ultimate properties were determined, and results used to predict the high heating value (HHV) of the agrowastes [6]. An investigation was carried out on the effect of carbon matter on peak crystallisation and stability using DSC [7]. It was discovered in the conclusion that carbon fibres did not change the global crystallization process. Oxidative degradation of isotactic polypropylene was evaluated using oxidation onset temperature (OOT) measurements [8]. It was concluded that OOT criterion was better than oxidation induction time (OIT) to evaluate the thermo-oxidative decomposition of isotactic polypropylene submitted to the environment during its useful lifetime.

The electrical and thermal properties of activated carbon are determined by structure; however, the different properties are interrelated [9]. In general, activated carbon fibers with high specific surface area exhibit low thermal conductivity and high electrical resistivity because of minimal available cross section of the electric current [9]. The thermal behavior of chemically activated carbon from agro-wastes as precursors for friction lining materials must be well understood for suitable applications. In this study, coconut and palm kernel shells which are readily available agrowastes in south-eastern region of Nigeria were used to produce chemically activated carbon with a view to characterize their proximate and thermal stability properties as precursors for organic friction linings.

2.0 METHODOLOGY

2.1 Materials

Materials employed to produce the activated carbon include coconut shells (CS), palm kernel shells (PKS), Calcium Chloride (CaCl_2), volumetric flask, distilled water, measuring scale, aluminium pot with lid, small ceramic pot with laboratory mortar, ball miller, ramming mass (castable), timer, thermocouple, and heat source.



Figure 1: Agrowaste biomass and the developed activated carbon samples

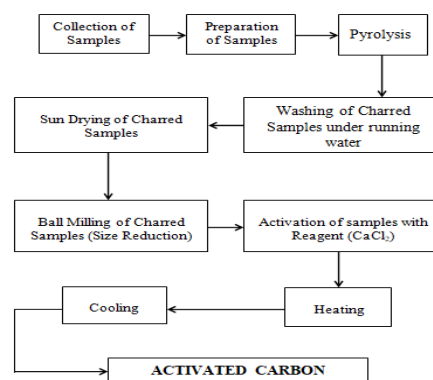


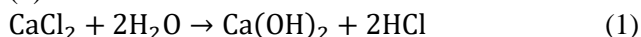
Figure 2: Flow chart for production of activated carbon

2.2 Production and Composition of Activated Carbons

The methods and processes employed to produce the coconut shell activated carbon (CSAC) and palm kernel shell activated carbon (PKSAC) were as reported by [10]. The chemistry of the preparation



involved the chemical reaction equation in Equation (1).



Mixing CaCl₂ with H₂O was an exothermic reaction. The PKSAC and CSAC produced as shown in Figure 1 were sieved into three different particle-sizes (60, 105, 150 μm) and collected into three different compositions as (X_{PKSAC} = 0% CSAC : 100% PKSAC, X_{PKSAC/CSAC} = 50% CSAC : 50% PKSAC, and X_{CSAC} = 100% CSAC : 0% PKSAC in volumes) for proximate property and thermal stability characterization. The process flow chart is shown in Figure 2.

2.3 Characterization of Activated Carbon

2.3.1 Proximate property characterization by thermogravimetric analysis (TGA)

Thermogravimetric analysis (TGA) was performed on the various samples to determine the moisture content, volatile matter, ash, and fixed carbon content following ASTM E1131-20 standard procedures [11]. Known sample weight (Table 1) of each particle size sample was subjected to TGA measurements by TA Analyser (TGA 2950, TA Instruments, USA) (Figure 3) at a heating rate 20°C/min, dynamic N₂ environment 50 mL/min and temperature range of 30 - 1000°C. Theoretically, the moisture content (MC), volatile matter (VM), ash (AC) and fixed carbon contents (FCC) (%) were calculated from the TGA thermogram using Equations (2) to (5), respectively for validation.

$$\text{MC} (\%) = \frac{(A-B)}{A} * 100 \quad (2)$$

where, A is mass of original sample (mg), and B is the mass of dried sample (mg) after first step decomposition.

$$\text{VM} (\%) = \frac{(B-C)}{A} * 100 \quad (3)$$

where, B is mass of dried sample after first step decomposition (mg), C is the mass of dried sample after second step decomposition (mg); A is mass of original sample (mg).

$$\text{AC} (\%) = \frac{D}{A} * 100 \quad (4)$$

where, D is the mass of ash (mg), A is the mass of the original sample (mg).

$$\text{FCC} (\%) = 100 - (\text{MC} + \text{VM} + \text{AC}) \quad (5)$$

2.3.2 Thermal stability characterization of activated carbon compositions

The thermal behaviour of samples at elevated temperatures were investigated by TGA according to ASTM E2550-21 [12] and by DSC following ASTM

D3418-21 [13] procedures. Measured sample weight (Table 1) of each sample was subjected to TGA as earlier stated in section 2.3.1. Also, known weight (Table 1) of each sample was subjected to a modulated differential scanning calorimetric analysis using MDSC 2920 (TA Instrument, USA) (Figure 4) at a heating rate 20°C/min, dynamic N₂ atmosphere 50 mL/min and temperature range 20 – 400°C. Similarly, two commercial friction linings materials, CB1 (Toyota, Japan) and CB2 (Superfit, China), purchased from an automobile parts market in Port Harcourt, Nigeria were subjected to the same tests above as controls.



Figure 3: TA analyzer 2950 used



Figure 4: MDSC 2920 analyzer used

Table 1: Mass of activated carbon samples used for thermal analysis

Activated carbon composition (% vol)	Particle size (μm)	TGA	DSC
		Mass of samples (mg)	Mass of samples (mg)
X _{PKSAC} = 0% CSAC:100% PKSAC	60	3.576	4.1
	105	3.482	2.4
	150	8.862	4.2
X _{PKSAC/CSAC} = 50% CSAC:50% PKSAC	60	2.863	3.8
	105	5.619	4.2
	150	5.308	3.4
X _{CSAC} = 100% CSAC:0% PKSAC	60	3.214	3.0
	105	5.757	3.6
	150	4.242	5.6

3.0 RESULTS AND DISCUSSION



3.1 Proximate analysis of 0% CSAC : 100% PKSAC Samples

The results of the proximate analysis of 0%CSAC:100%PKSAC samples based on their particle size are discussed in sections 3.1.1 to 3.1.3 and compared with the control samples in Table 2.

3.1.1 60 μm of 0% CSAC : 100% PKSAC Sample

Figure 5 shows the TGA thermogram of 60 μm of 0% CSAC : 100% PKSAC sample. It was observed that at 72.57°C, 6.4% MC of 60 μm 0% CSAC : 100% PKSAC sample evaporated remaining 93.54%. Within the temperature range of 72.57°C to 114.28°C, 3.9% VM was released while 4.8% AC was recorded at 991.29°C. The 60 μm of 0%CSAC:100%PKSAC sample showed the highest FCC of 84.76% with smaller volatile matter, lower ash and moisture content implying a better thermal stability which is evident by its optimum degradation temperature (ODT). This corroborates other published results [21]. Lower MC (%) with smaller particle size of materials has been found to improve mechanical properties [15].

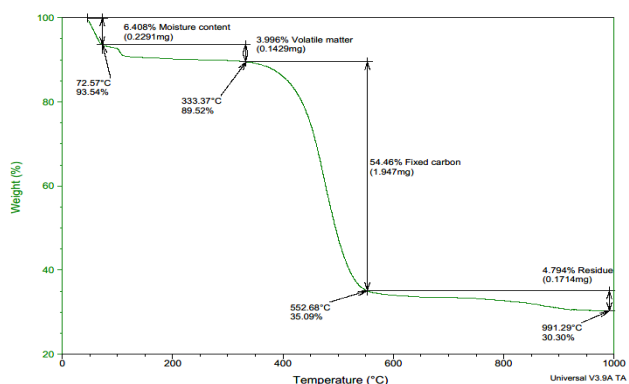


Figure 5: TGA of 60 μm of 0% CSAC : 100% PKSAC sample

3.1.2 105 μm of 0% CSAC : 100% PKSAC Sample

Figure 6 shows the thermogram of 105 μm of 0% CSAC : 100% PKSAC sample. It was observed that at 72.57°C, 7.8% MC evaporated remaining 92.22%. Between the temperature range of 72.57°C to 117.85°C, 4.884% VM was released while 4.218% AC was recorded at 896.46°C. From this study, 105 μm of 0% CSAC : 100% PKSAC sample had higher FCC of 83.096%, smaller VM, lower AC and MC which suggests a better thermal stability. This corroborates other published finding [21] which reported that higher fixed carbon content is suggestive of greater heating value, lower AC, VM and MC. As MC (%) increased with increase in particle size, the thermal stability measured by ODT reduced, hence, mechanical properties are reduced. Finer particle accumulates lesser moisture which improves the

mechanical properties. This agrees with another research finding [15].

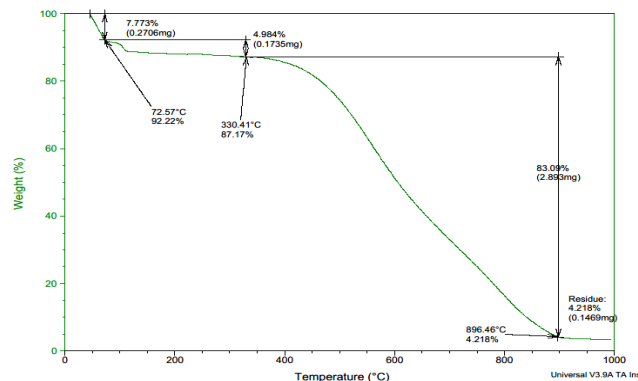


Figure 6: TGA of 105 μm of 0% CSAC : 100% PKSAC sample

3.1.3 150 μm of 0% CSAC : 100% PKSAC Sample

Figure 7 shows the thermogram of the proximate analysis of 0% CSAC : 100% PKSAC sample with 150 μm particle size. It was observed that at 88.87°C, 11.48% MC evaporated remaining 84.47%. Between the temperature range of 88.87°C to 128.57°C, 5.06% VM was released while 6.35% AC was recorded at 914.24°C. High MC in 150 μm 0% CSAC : 100% PKSAC sample generally decreased its heating value. Lesser moisture is required to achieve several purposes in friction materials and thermal applications [20]. Also, higher MC affects the storability of the activated carbon samples. The low VM content of this sample revealed its capability of producing high carbon content and thermal stability as lower VM suggest higher fixed carbon. Also, lower AC improves the FCC thereby increasing the heat value of the sample. Hence, 150 μm of 0% CSAC : 100% PKSAC sample showed a 77.06% FCC which implied that this sample exhibited good thermal properties - ODT [23, 24] suitable for development of friction lining material.

Comparing the proximate properties in Figure 5, Figure 6 and Figure 7, MC and VM increased with particle sizes for 0% CSAC : 100% PKSAC samples. This trend affects the material mechanical properties. Lower MC leads to improved mechanical properties. This corroborates other published findings [15, 18]. Larger particle granules have high pores which can accumulate more moisture thereby reducing its physico-mechanical properties. Low VM was observed in the 0% CSAC : 100% PKSAC samples with respect to particle sizes in the order; 60 μm < 105 μm < 150 μm (being highest for 150 μm). It was observed that particle size determined the thermal stability of the activated carbon which is in line other finding [17]. The AC showed fluctuating trends due to



variations in the moisture, particle size, temperature, material type and FCC. This is in tandem with other results [22, 23]. Whereas FCC showed a decreasing trend with particle size increase finer particles exhibited better thermal properties.

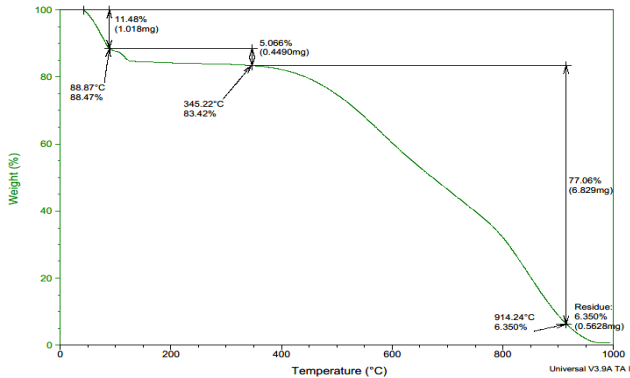


Figure 7: TGA of 150 µm of 0% CSAC : 100% PKSAC sample

3.2 Proximate analysis of 50% CSAC : 50% PKSAC Samples

The results of the proximate analysis of 50% CSAC : 50% PKSAC samples based on their particle sizes are discussed in sections 3.2.1 to 3.2.3 and compared with the control samples in Table 2.

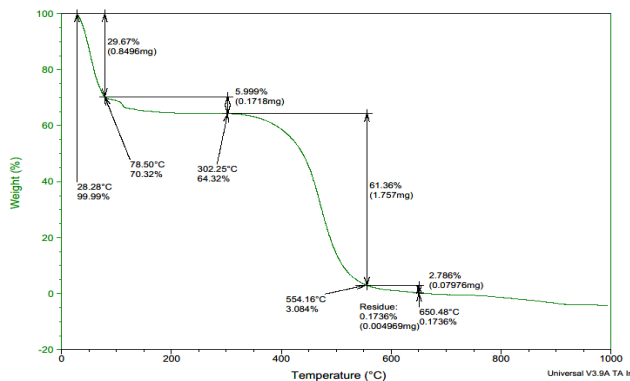


Figure 8: TGA of 60 µm of 50% CSAC : 50% PKSAC sample

3.2.1 60 µm of 50% CSAC : 50% PKSAC Sample

Figure 8 shows the thermogram of the proximate analysis of 50% CSAC : 50% PKSAC sample with 60 µm particle size. At 78.50°C, 29.67% MC of the sample evaporated remaining 70.32%. Between the temperature range of 78.50°C to 302.25°C, 5.9% VM was released while 0.1736% AC was recorded at 650.48°C resulting to FCC of 64.15%. This amount of FCC was evidenced by its high MC. Higher MC contributed greatly to low FCC of this sample, influencing ODT relative to other particle size of same composition. This confirmed that samples with higher MC yield lower carbon content. It has been reported

that the higher the FCC, the smaller the VM, the lower the AC and MC and the better the thermal quality of sample [21].

3.2.2 105 µm of 50% CSAC : 50% PKSAC sample

Figure 9 shows the thermogram of the proximate analysis of 50% CSAC : 50% PKSAC sample with 105 µm particle size. It was observed that at 84.43°C, 22.997% MC evaporated remaining 76.99%. Between the temperature range of 84.43°C to 336.33°C, 4.869% VM was released while 1.474% AC was recorded at 760.13°C. The 105 µm of 50% CSAC : 50% PKSAC sample showed FCC of 70.42% implying that as MC reduced, FCC increased indicating improved ODT when compared with the developed (60 µm of 50% CSAC : 50% PKSAC) sample with 29.67% MC.

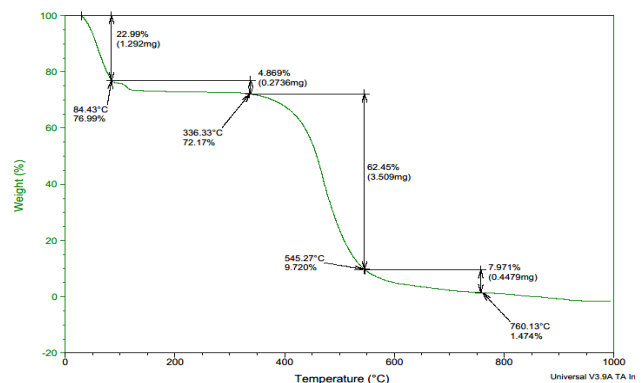


Figure 9: TGA of 105 µm of 50% CSAC : 50% PKSAC sample

3.2.3 150 µm of 50% CSAC : 50% PKSAC Sample

Figure 10 shows the thermogram of 50% CSAC : 50% PKSAC sample with 150 µm particle size. It was observed that at 81.46°C, 5.96% MC in the sample evaporated remaining 93.95%. Within the temperature range of 81.46°C to 142.85°C, 6.95% VM was released while 13.27% AC was recorded at 911.28°C resulting to FCC of 73.87%. In general, the proximate analyses of the hybrid 50% CSAC : 50% PKSAC samples showed that its MC decreased with increase in particle size. The lower moisture content observed with the 150 µm of 50% CSAC : 50% PKSAC sample maybe as a result of the higher percentage of fixed carbon and ash content present. This result is consistent with other works [16, 19] but does not agree with another work [15] which reported that MC increase with increase in particle size. The FCC and AC increased with increase in particle size, but VM of the hybrid 50% CSAC : 50% PKSAC samples showed a fluctuating trend with particle size which is consistent with other published results [19]. The 150 µm of 50% CSAC : 50% PKSAC recorded higher FCC, smaller VM, lower AC, and MC implying a better thermal stability than other samples with



400.5°C ODT which agrees with other findings [21, 25].

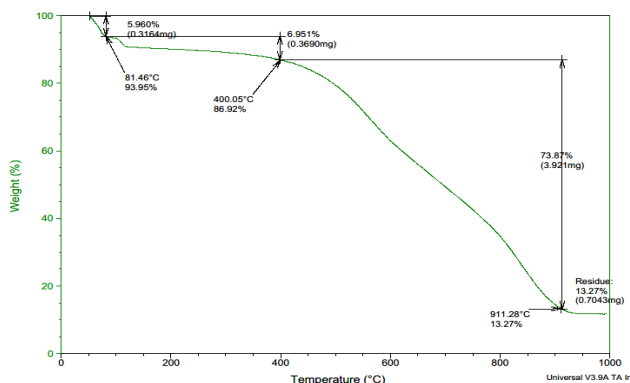


Figure 10: TGA of 150 µm of 50% CSAC : 50% PKSAC sample

3.3 Proximate analysis of 100% CSAC : 0% PKSAC Samples

The results of the proximate analysis of 100% CSAC : 0% PKSAC samples based on the particle sizes are discussed in sections 3.3.1 to 3.3.3 and compared with the control samples in Table 2.

3.3.1 60 µm of 100% CSAC : 0% PKSAC Sample

The thermogram in Figure 11 shows the proximate analysis result of 100% CSAC : 0% PKSAC sample with 60 µm particle size. From Figure 11, it was observed that at 78.5°C, 20.67% moisture evaporated remaining 79.49%. Within the temperature range of 78.5°C to 114.28°C, 5.363% VM was released while 0.042% AC was recorded at 997.91°C yielding a fixed carbon content of 73.87%. The MC influenced the FCC of sample which reduced the ODT.

3.3.2 105 µm of 100% CSAC : 0% PKSAC sample

Figure 12 shows the thermogram of the proximate analysis of 100% CSAC : 0% PKSAC sample with 105 µm particle size. It can be observed that at 94.80°C, 30.57% moisture evaporated remaining 69.43%. From 94.80°C to 128.57°C, 4.842% VM was released while 6.603% AC was recorded at 872.75°C with FCC of 57.77%. This amount was low compared to that of 60 µm particle size. This was due to the high MC obtained as particle size increased showing consistency with other published works [23, 24].

3.3.3 150 µm of 100% CSAC : 0% PKSAC Sample

Figure 13 shows the thermogram of 100% CSAC : 0% PKSAC sample with 150 µm particle size. It can be observed that at 88.87°C, 14.66% MC evaporated remaining 84.46%. Within the temperature range of 88.87°C to 142.86°C, 6.896% VM was released while 0.575% AC was recorded at 817.92°C yielding FCC of 77.39%. This FCC was better than the FCC value

for 105 µm of 100% CSAC : 0% PKSAC sample. Comparing the proximate properties for all 100% CSAC : 0% PKSAC samples, it was observed that MC, VM, AC, and FCC showed fluctuating trend with respect to particle size. The MC increased from 20.67% for 60 µm to 30.57% for 105 µm but dropped to 14.66% for 150 µm. The VM was higher for 150 µm than those of other particle sizes. 150 µm of 100% CSAC : 0% PKSAC sample recorded higher FCC, smaller VM, lower AC, and MC implying a better thermal quality with good heating value corroborating other findings [21, 25]. This higher FCC of the sample is evident by the ODT.

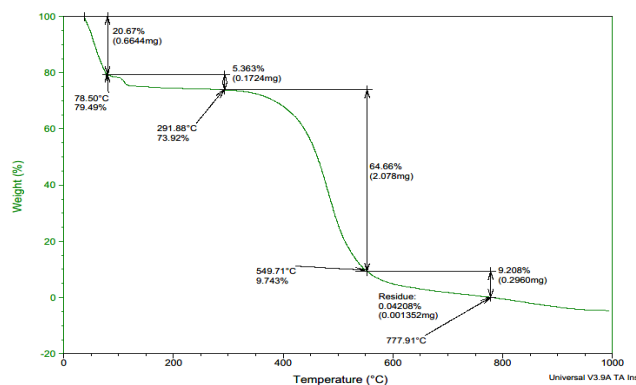


Figure 11: TGA of 60 µm of 100% CSAC : 0% PKSAC sample

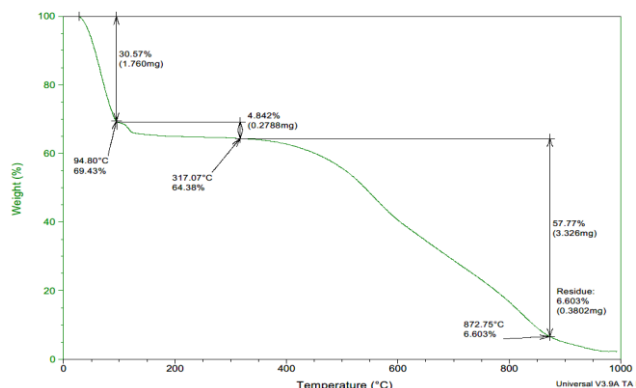


Figure 12: TGA of 105 µm of 100% CSAC : 0% PKSAC sample

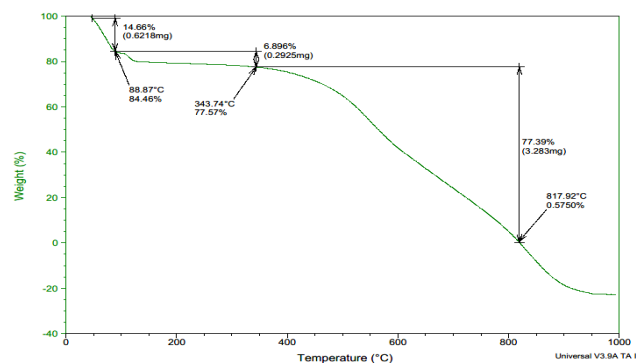


Figure 13: TGA of 150 µm of 100% CSAC : 0% PKSAC sample



Table 2: Proximate properties of the activated carbon compositions and controls

Activated Carbon Compositions	Particle Size (µm)	Proximate parameters			
		Moisture Content (%)	Volatile Matter (%)	Fixed Carbon Content (%)	Ash Content (%)
0% CSAC : 100% PKSAC	60	6.04	3.99	84.8	4.79
	105	7.77	4.98	83.09	4.22
	150	11.48	5.07	77.06	6.35
	CB1	2.27	2.18	45.47	48.86
	CB2	1.92	1.49	37.21	58.07
50% CSAC : 50% PKSAC	60	29.67	5.99	64.15	0.17
	105	22.99	4.87	70.42	1.47
	150	5.96	6.95	73.87	13.27
	CB1	2.27	2.18	45.47	48.86
100% CSAC : 0% PKSAC	60	1.92	1.49	37.21	58.07
	105	20.67	5.36	73.87	0.04
	150	30.57	4.84	57.77	6.60
	CB1	14.66	6.89	77.39	0.57
	CB2	2.27	2.18	45.47	48.86
	CB2	1.92	1.49	37.21	58.07

3.4 Thermal behaviour of friction lining materials

The thermal behaviour of the activated carbon friction linings developed were studied by TGA and DSC to determine the effects of composition type and particle size on the ODT and oxidation temperature (OT) in comparison with two commercial friction lining materials (CB1 and CB2) used as controls. The ODT is the temperature at which the maximum degradation rate is observed for the main degradation step on the thermogram while the onset oxidative temperature (OOT) is a relative measure a material resistance to oxidative. The higher the OOT value the more stable the material.

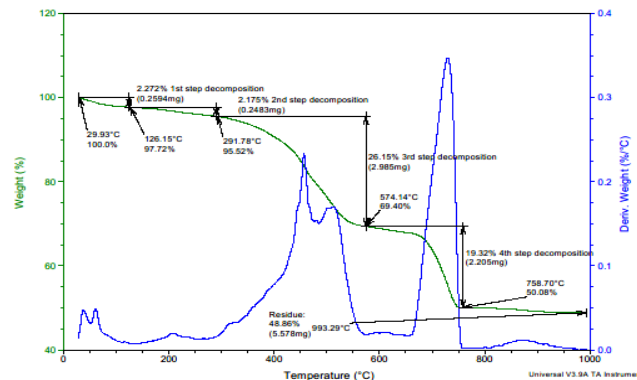


Figure 14: TGA thermograms of control friction lining CB1

3.4.1 TGA / DSC of the control friction linings

Figure 14 shows the thermogram of the control friction lining sample CB1. It was observed that the sample entered TG measurement at 29.93°C with the first step decomposition at 126.15°C with 2.272% of moisture evaporation. 2.175% VM was found to have decomposed during the second step at 291.79°C. The ODT was observed to be 291.79°C. Third step and fourth step decompositions were completed at

574.14°C and 758.70°C, respectively, leaving a residue of 48.86% at 993.29°C.

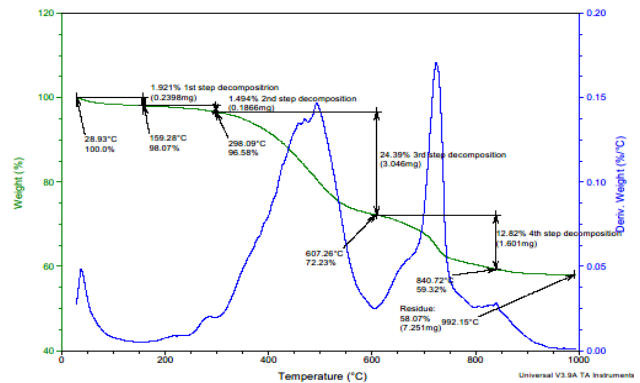


Figure 15: TGA thermograms of control friction lining CB2

For CB2 sample thermogram in Figure 15, the measurement commenced at 28.93°C with first step decomposition at 159.28°C and 1.921% moisture evaporation. 1.494% VM decomposed at the second step at 298.09°C. For this control sample ODT was observed to be 298.09°C. Third step and fourth step decompositions were completed at 607.26°C and 840.72°C, respectively, leaving a residue of 58.07% at 992.15°C. Though ODT of the two control samples are comparable, CB2 is more stable than CB1.

3.4.2 TGA / DSC of 0% CSAC : 100% PKSAC Sample

Figure 16 shows the ODT of the developed 0% CSAC : 100% PKSAC samples and the control samples. It can be observed that ODTs of the developed samples showed higher thermally stability than the two control samples. Also, as particle size increases, ODT increases. This corroborates other published results [14], it was attributed to higher surface area of smaller granules, leading to decreased yielding and increase in ODT. This was observed in all developed samples. The 60 µm of 0% CSAC : 100% PKSAC samples showed 14% and 11%, 105 µm of 0% CSAC : 100% PKSAC sample showed 16.5% and 14% while 150µm 0% CSAC : 100% PKSAC sample showed 18.3% and 15.8% better performance than CB1 and CB2, respectively. Hence, the developed 0% CSAC : 100% PKSAC samples with different particle sizes can be suitable precursors for organic friction linings. Figure 17 shows OOT based on the DSC results obtained for 0% CSAC : 100% PKSAC which was comparable with CB1 and CB2. Based on OOT, the developed 0% CSAC : 100% PKSAC samples of different particle sizes showed superior oxidative stability than CB2. On the OT of 0% CSAC : 100% PKSAC activated carbon composition depicted in Figure 16, OT increased as particle size increased with a slight drop

at 150 μm . This activated carbon samples compared favorably with the control sample CB1.

3.4.3 TGA / DSC of 50% CSAC : 50% PKSAC Sample

Figure 16 shows the ODT 50% CSAC : 50% PKSAC samples and the control samples. It was observed that the ODT of the developed samples showed higher thermal stability than the two control samples. Also, as particle size increased, the ODT increased. The 60 μm 50% CSAC : 50% PKSAC sample showed 3.58% and 1.39%, 105 μm 50% CSAC : 50% PKSAC sample showed 15.3% and 12.83% while 150 μm 50% CSAC : 50% PKSAC sample showed 37.1% and 34.20% better performance than CB1 and CB2, respectively. Hence, the developed samples of 50% CSAC : 50% PKSAC composition with different particle sizes can be suitable precursors for friction linings. Figure 17 shows the OOT of the 50% CSAC : 50% PKSAC samples, where the OOTs were found to be comparable with those of CB1 and CB2. Based on OOT, the developed samples of 50% CSAC : 50% PKSAC composition with different particle-sizes showed better oxidative stability than CB2 except for 105 μm particle-size sample which was less than CB1 and CB2 with OOT of 177.48 $^{\circ}\text{C}$. On the OT of 50% CSAC : 50% PKSAC sample depicted in Figure 16, OT decreased as particle size increased. This sample compared favorably with the control sample CB1.

3.4.4 TGA / DSC of 100% CSAC : 0% PKSAC Sample

Figure 16 shows ODT of 100% CSAC : 0% PKSAC samples and control-samples. It was observed that ODT of the developed samples showed higher thermally stability than the two control samples. Also, as particle-size of samples increased, ODT increased. The 60 μm of 100% CSAC : 0% PKSAC sample showed 3.4% and -2.1%, 105 μm of 100% CSAC : 0% PKSAC sample showed 8.7% and 6.4% while 150 μm of 100% CSAC : 0% PKSAC sample showed 17.8% and 15.3% better performance than CB1 and CB2, respectively. Hence, the developed samples with different particle sizes can be suitable precursors for organic friction linings. Similarly, Figure 17 shows OOT of 100% CSAC : 0% PKSAC samples with OOT comparable to the control samples. Based on OOT, the developed samples with different particle-sizes showed superior oxidative stability than CB2. Also, the 60 μm of 100% CSAC : 0% PKSAC sample showed better oxidative stability than CB1 and CB2 with OOT of 218.1 $^{\circ}\text{C}$. On the OT of the 100% CSAC : 0% PKSAC samples depicted in Figure 18, OT increased as particle size increased. This sample compared favorably with the control sample CB1.

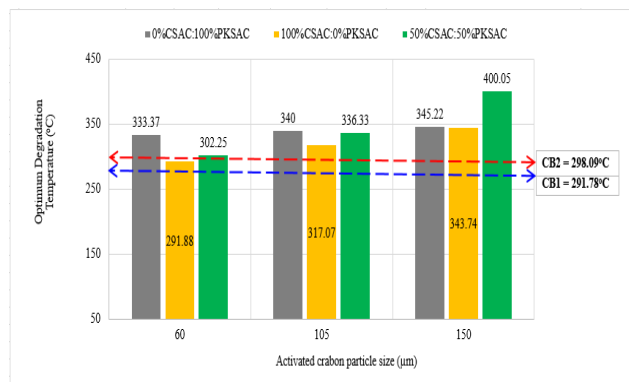


Figure 16: Optimum degradation temperature (ODT) of developed samples and the control

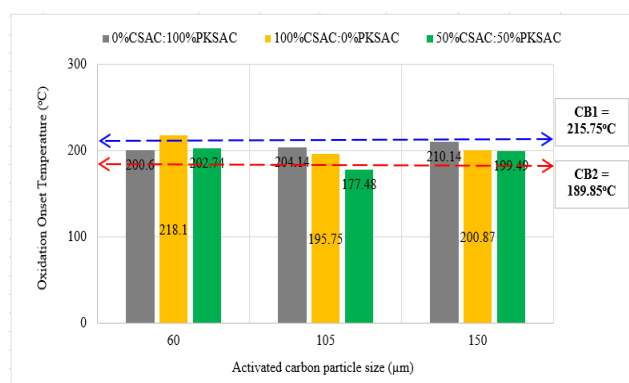


Figure 17: Oxidation onset temperature (OOT) of developed samples and the control

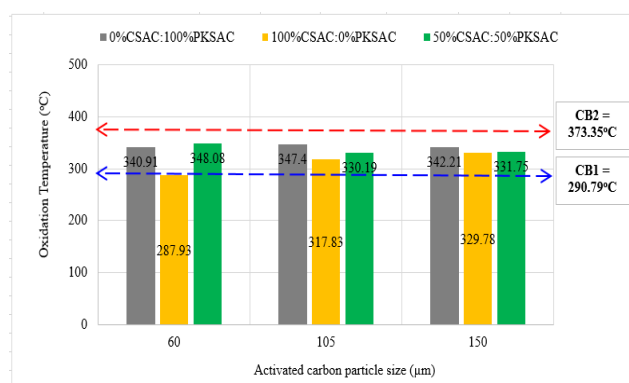


Figure 18: Oxidation temperature (OT) of developed samples and control samples

4.0 CONCLUSION

Proximate property of 0% CSAC : 100% PKSAC samples showed that moisture content and volatile matter increased as particle-size increased. Ash content recorded fluctuating trends with particle size, whereas the fixed carbon content showed a reverse trend with particle size. The moisture content of 100% CSAC : 0% PKSAC fluctuated with increasing particle size; increasing from 20.67% for 60 μm to 30.57% for 105 μm but dropping to 14.7% for 150 μm . Volatile matter was highest for 150 μm among other



particle sizes. 0% CSAC : 100% PKSAC samples had its ODT increasing with particle size which was superior to the two control samples. The heat flow pattern of 0% CSAC : 100% PKSAC samples showed comparable OOT with the control samples, but better than CB2. The ODT of 50% CSAC : 50% PKSAC samples showed higher thermal stability than the two control samples. The ODT trends showed linear relationship with particle size; even as the 150 μm of 50% CSAC : 50% PKSAC sample exhibited best ODT with 37.1%, 34.2% than CB1 and CB2, respectively.

This was followed by 0% CSAC : 100% PKSAC sample with 18.3%, 15.8% while 100% CSAC : 0% PKSAC had 17.8%, 15.3% performance than CB1 and CB2, respectively. The OOT of all samples compared well with CB1 and CB2 showing better oxidative stability except for 105 μm of 50% CSAC : 50% PKSAC sample which was less stable than CB1 and CB2 with OOT of 177.48°C. For 100% CSAC : 0% PKSAC samples, the ODT showed higher thermally stability than the two control samples. The 60 μm of 100% CSAC : 0% PKSAC sample showed better oxidative stability than control samples with 218.1°C OOT. Although CB2 had an oxidation temperature (OT) value of 373.35°C, all the activated carbon compositions compared well with CB1. From these findings, the developed activated carbon compositions and particle sizes can be suitable precursors for organic friction lining materials.

5.0 ACKNOWLEDGEMENT

The authors wish to thank PGE Applied Resources Material Laboratory Imo state, Nigeria for collaboration in conducting some of the tests.

6.0 CONFLICT OF INTEREST

The authors declare that there is no conflict of interest.

REFERENCES

[1] Chung, D. D. L. "Thermal analysis of carbon fibre polymer-matrix composites by electrical resistance measurement", *Thermochimica Acta*, 364, 121-132, 2000.

[2] Pandolfo, A. G., and Hollenkamp, A. F. "Carbon properties and their role in supercapacitors", *Journal Power Sources*, 157 (01), 11-27, 2006.

[3] Maria de Fatima, S., Adekunle, M. A., Muhammad, M. J., João, A. S., and Farid, N. A. "Preparation of activated carbon from babassu endocarp under microwave radiation by physical activation", *IOP Conference. Ser.: Earth Environ. Science*, 105, 012116, 2018.

[4] Brown, M. E. "Introduction to Thermal Analysis: Techniques and Application", *Chapman & Hall, New York*, 25, 1988.

[5] Radic, D. B., Miroslav, M. S., Marko, O. O., and Aleksandar, M. J. "Thermal analysis of physical and chemical change occurring during regeneration of activated carbon", *Thermal Science*, 21 (02), 1067-1081, 2017.

[6] Alejandra, S., Anabel, F., German, M., and Rosa, R. "Prediction of regional agro-industrial wastes characteristics by thermogravimetric analysis to obtain bioenergy using thermal process", *Energy Exploration & Exploitation*, 37 (01), 544-557, 2019.

[7] De-Almeida, O., Besnard, E., and Bernhart, G. "DSC investigation of the influence of carbon content on peek crystallisation and stability", in *Proc. 19th International Conference on Composite Materials (ICCM 19)*, Montreal, Quebec, Canada, July 28 -August 2, 2013, 8625.

[8] Volponi, J. E., Mei, L. H. I., and Rosa, D. S. "Use of Oxidation Onset Temperature Measurements for Evaluating the Oxidative Degradation of Isotactic Polypropylene", *Journal of Polymers and the Environment*, 12 (01), 11-15, 2004.

[9] Huang, Y. "Electrical and thermal properties of activated carbon fibres" in "Activated Carbon Fiber and Textiles", 179-190, 2017.

[10] Akuwueke, L. M., Ossia, C. V., and Nwosu, H. U. "Optimisation of the mechanical properties of chemically activated carbon composites in organic friction linings by Box-Behnken design", *Proceedings of Engineering Sciences (PES)*, 04 (02), 191-202, 2022.

[11] ASTM, "Standard test method for compositional analysis by thermogravimetry", ASTM E1131-20, 2020.

[12] ASTM, "Standard test method for thermal stability by thermogravimetry", ASTM E2550-21, 2021.

[13] ASTM, "Standard test method for transition temperatures and enthalpies of fusion and crystallization of polymers by differential scanning calorimetry", ASTM D3418-21, 2021.

[14] Navid, S., and Mohammad, N. L. "Effects of Powder Activated Carbon Particle-size on Adsorption Capacity and Mechanical Properties of the Semi Activated Carbon Fiber", *Fibers and Polymers*, 16 (03), 543-549, 2015.

[15] Ossia, C.V., Big-Alabo, A., and Ekpruke, E. O. "Effect of Particulate Grain Size on the



- Physicomechanical Properties of Green Automotive Brake Pads from Waste Coconut (Cocosnucifera L.) Shells”. *Advances in Manufacturing Science & Technology*, 44 (4), 135-144, 2020.
- [16] Lori, J. A., Afolabi, L., and Lawal, A. O. “Proximate and Ultimate Analyses of Palm Kernel Shell as Precursor for Activated Carbon”, *Journal of Harmonized Research in Applied Sciences*, 5 (4), 181-186, 2017.
- [17] Fauzia, E. A., and Purnama, H. “The effect of particle size on the characterization of activated carbon from tropical black bamboo (Gigantochloa Atrovioleacea)”, *Techno (Jurnal Fakultas Teknik Universitas Muhammadiyah Purwokerto)*, 22 (2), 99, 2021.
- [18] Saeidi, N., and Lotfollahi, M. N. “Effects of powder activated carbon particle size on adsorption capacity and mechanical properties of the semi activated carbon fibre”, *Fibers and Polymers*, 16 (3), 543-549, 2015.
- [19] Abdulganiyu, B., Edeoja, A. O., Ibrahim, J. S., and Kwaghger, K. A. “Performance Evaluation of Raphia Palm (R. vinifera) Seeds Briquettes with Cassava Starch as Binder”, *Journal of Energy Research and Reviews*, 11 (2), 36-62, 2022.
- [20] Ivanova, T., Havrland, B., Hutla, P., and Muntean, A. “Drying of cherry tree chips in the experimental biomass dryer with solar collector”, *Res. Agr. Eng.*, 58, 16-23, 2012.
- [21] Inegbedion, F. “Estimation of the Moisture Content, Volatile Matter, Ash Content, Fixed Carbon and Calorific Values of Saw dust Briquettes”, *MANAS Journal of Engineering*, 10 (1), 18-19, 2022.
- [22] Zaki, B. Z., Appalasaamy, S., Nor, M. M., and Rak, A. E. “Effect of Temperature on Moisture, Ash and Crude Fat Content in Etak (Corbicula fluminea) Tissue via Modified Oven Smoking Method”, *2nd International Conference on Tropical Resources and Sustainable Sciences IOP Conf. Ser.: Earth and Environmental Science*, 549 (012056), 1-7, 2020.
- [23] Coelho, P. S., Otavio Augusto, P., Ferreira de, O. M., Albuquerque, S. G., Monteiro, R. V., and Farias, R. L. “The effect of temperature on corn straw ash production as supplementary cementitious material”, *Revista Científica Multidisciplinar Núcleo do Conhecimento*, 03, 76-112, 2023.
- [24] Kotoulek, P., Bozikova, M., Hlavac, P., Petrovic, A., Csillag, J., Malinek, M., and Bilcık, M. “Effect of different moisture contents on the thermal properties of wood”, *Journal on Processing and Energy in Agriculture*, 23 (01), 24-26, 2019.
- [25] Bastakoti, N., Dhital, H. C., and Aryal, A. “Study of effects of temperature and residence time on calorific value of torrefied biomass”, *International Journal of Research in Engineering and Technology*, 07 (10), 31-35, 2018.

